958–969 *Nucleic Acids Research, 2011, Vol. 39, No. 3* *Published online 6 October 2010*
doi:10.1093/nar/gkq882

Amplification of a plasmid bearing a mammalian replication initiation region in chromosomal and extrachromosomal contexts

Seiyu Harada, Naoki Sekiguchi and Noriaki Shimizu*

Graduate School of Biosphere Science, Hiroshima University, Higashi-Hiroshima 739-8521, Japan

Received May 15, 2010; Revised September 17, 2010; Accepted September 19, 2010

ABSTRACT

Amplified genes in cancer cells reside on extrachromosomal double minutes (DMs) or chromosomal homogeneously staining regions (HSRs). We used a plasmid bearing a mammalian replication initiation region to model gene amplification. Recombination junctions in the amplified region were comprehensively identified and sequenced. The junctions consisted of truncated direct repeats (type 1) or inverted repeats (type 2) with or without spacing. All of these junctions were frequently detected in HSRs, whereas there were few type 1 or a unique type 2 flanked by a short inverted repeat in DMs. The junction sequences suggested a model in which the inverted repeats were generated by sister chromatid fusion. We were consistently able to detect anaphase chromatin bridges connected by the plasmid repeat, which were severed in the middle during mitosis. *De novo* HSR generation was observed in live cells, and each HSR was lengthened more rapidly than expected from the classical breakage/fusion/bridge model. Importantly, we found massive DNA synthesis at the broken anaphase bridge during the G1 to S phase, which could explain the rapid lengthening of the HSR. This mechanism may not operate in acentric DMs, where most of the junctions are eliminated and only those junctions produced through stable intermediates remain.

INTRODUCTION

Amplification of oncogenes or drug resistance genes plays a pivotal role in malignant transformation of human cells. Amplified genes are frequently localized at either the chromosomal homogeneously staining region (HSR) or the extrachromosomal element [for recent review, see (1,2)]. The size of such extrachromosomal elements may vary significantly from the submicroscopic episome to the microscopically visible double minutes (DMs). DMs are several megabase pairs in length and are composed of genome-derived circular acentric and atelomeric DNA. The 'episome model' of gene amplification attempts to explain the development of DMs and HSRs. In this model, episomes excised from the chromosome arm multimerize to produce DMs, which in turn generate HSR in the chromosome arm (3).

We previously found that a plasmid bearing both a mammalian replication initiation region (IR) and a nuclear matrix attachment region (MAR) was efficiently amplified to several thousand copies per cell in human cancer cells, and that the amplified sequences appeared as DMs and/or HSR (4,5). Because the sequences for IR or MAR are scattered throughout the genome, the IR/MAR-bearing plasmid may represent the episome excised from the chromosome arm, and may reproduce the episome model efficiently in cultured mammalian cells. For these reasons, we have used this experimental system extensively for uncovering mechanisms of gene amplification (4,6,7) and for analyzing the intracellular behavior of DMs or HSRs in live cells (6,8–10). The IR/MAR plasmid has also been used successfully as a tool in basic studies of nuclear functional structure (11,12).

Our previous studies suggested a mechanism to explain how the IR/MAR plasmid might mimic gene amplification (6). The IR/MAR plasmid is multimerized to a large circular molecule in which the plasmid sequences are arranged as a direct repeat (4). If the multimerization progresses significantly, the extrachromosomal circles may be microscopically visible as DMs. Alternatively, the circular plasmid repeat may integrate within pre-existing DMs that are generated during oncogenesis (6), because the recombination between the

*To whom correspondence should be addressed. Tel: +81 824 24 6528; Fax: +81 824 24 0759; Email: shimizu@hiroshima-u.ac.jp

extrachromosomal molecules appears frequent. If a double-strand breakage arises in the DMs, they may be eliminated from the cells (8,13), or they may be integrated into the chromosome arm. If the plasmid repeat is broken at the chromosome arm, the breakage-fusion-bridge (BFB) cycle may be initiated at that site, and a long HSR composed of plasmid sequences may be generated (6). The BFB cycle model was proposed by B. McClintock about six decades ago (14), and has been frequently used to explain gene amplifications and gross chromosomal alterations in tumor cells (1,15–17). According to this model, the generation of a chromatin bridge from a dicentric chromatid and its breakage during anaphase plays a central role in the lengthening of the HSR. The broken chromosome, after replication and end-to-end fusion of sister chromatids during subsequent interphase, again generates a dicentric chromatid. This results in a continuing cycle of breakage and fusion, and selective pressure may lead to amplification of genes near the initial break. Previously, we observed that the HSR formed an anaphase bridge in live cells, and that it broke almost at the midpoint between two kinetochores (6).

Using the IR/MAR plasmid system, we have shown that the DMs are composed of ordered, direct plasmid repeats, whereas the repeats were partially disturbed in HSR (4). Interestingly, these studies identified an instance where the DM had a recombined plasmid sequence, which might be produced by the re-joining between two breaks in the plasmid direct repeat. In this article, we extended these findings and revealed many recombined sequences in DMs and HSRs, which were related to the progression of gene amplification. The live-cell observation of HSR generation suggested that HSR length increased more rapidly than expected from the classical model. Unscheduled DNA synthesis was consistently observed at the broken bridge after the mitosis, which could lengthen the HSR rapidly. These findings significantly improved our understanding of gene amplification in chromosomal and extrachromosomal contexts.

MATERIALS AND METHODS

Plasmids

The origin and structure of pSFVdhfr, pΔBN.AR1, pΔB.AR1 (4) and pCMV-d2EGFP (7) have been previously described. Plasmids pHS-I and pHS-D (18) with inverted and direct repeats, respectively, of the human *Alu* sequence, separated by 12-bp spacers, were a kind gift from Dr Kirill Lobachev (Georgia Institute of Technology). The inverted and direct repeat *Alu* repeats from these plasmids were excised by *Xho* I/*Bam* HI digestion, and were inserted at the *Bam* HI/*Nru* I site of pΔB.AR1 plasmid to obtain pΔBN.AR1.Alu-I and pΔBN.AR1.Alu-D, respectively. The plasmids were cloned in *Escherichia coli* SURE2 competent cells (Agilent Technologies Inc.). pΔBN.AR1.Alu-S, which has single copy *Alu*, was obtained by digesting pΔBN.AR1.Alu-D with *BamH* I/*Sal* I, to delete one of the two *Alu* sequences.

Cell culture, plasmid transfection and cytochemical procedures

Human COLO 320DM (CCL 220) neuroendocrine tumor cells were maintained as previously described (19). All transfections were performed using the Gene Porter 2 lipofection kit (Genlantis Co. CA). Stable transformants were selected using 5 μg/ml blasticidine (Funakoshi, Co. Tokyo, Japan), and continuously grown in this concentration of drug. More than 1 month after the transfection, the polyclonal transformant was analyzed by FISH to determine the location of plasmid sequence, as described (19). At that time, total cellular DNA was isolated and subjected to PCR analysis. Monoclonal clone 12 or 22 cells were obtained by transfecting the pSFVdhfr plasmid into COLO 320DM cells, and these cells had amplified plasmid sequences only at DMs or HSRs, respectively (4,11). For the simultaneous detection of HSRs and DNA synthesis, we treated the HSR-CFP cells (see below) with 0.4 μg/ml of nocodazole for 10 h to partially synchronize the cell cycle. They were then released into fresh medium for 1–6 h, and treated with 20 μg/ml BrdU during the last hour. We fixed the cells with paraformaldehyde (PFA), and detected the incorporated BrdU using a buffer containing DNase and anti-BrdU mouse monoclonal antibody, using the same protocol as described previously (10).

PCR amplification of type 1 or 2 structure and base sequencing

We synthesized 64 different PCR primers (Tsukuba oligo service, co., Japan) along the plasmid sequence (Supplementary Figure S1). The sequences are listed in Supplementary Table S1. In order to amplify the type 1 or 2 structures, 140 or 75 sets of primers, respectively, were chosen (Supplementary Table S2). Total cellular DNA was isolated as described (20). PCR was performed using the following condition. The 20-μl reaction mixture contained 1× Blend *Taq* Buffer (Toyobo Co., Osaka, Japan), 200 μM dNTP (Toyobo), 0.12 unit of Blend *Taq* Plus (Toyobo), 1 μM primer and 15 ng of total cellular DNA. The PCR condition for type 1 structure was 35 cycles at 94°C for 30 s, 60°C for 30 s and 72°C for 60 s. The PCR condition for type 2 structure was 35 cycles at 94°C for 30 s, 60°C for 30 s and 72°C for 3 min. In order to amplify the palindrome or the inverted repeat with short spacer sequence, we treated the template DNA with bisulfite to convert unmethylaed cytosine to uracil, using the EpiTect bisulfite kit (Qiagen Inc.) according to the manufacturer's recommendations. Four sets of primers (noted as a to d) for such PCR were specially designed along the entire plasmid, where original C was substituted by T. The primers are listed in Supplementary Table S3. The PCR product was cloned using pGEM-T Easy Vector Systems (Promega) and *E. coli* DH5α (TOYOBO, Co., Osaka). DNA for sequencing was directly amplified from the *E. coli* colony by PCR using Blend *Taq* Plus. The product was purified by passing

it through the DTR gel filtration cartridge (Edge BioSystems, MD), and was analyzed by the ABI PRISM dGTP BigDye terminator ready reaction kit (Applied Biosystems) and the ABI PRISM 310 genetic analyzer (Applied Biosystems).

Detection of HSR in live cells

'HSR-CFP cells', in which LacO-tagged HSR was visualized by the binding of LacR-CFP fusion protein, were described in our previous article (10). Each cell has two or three large HSRs. Time-lapse observation shown in Figure 5 was done using the same facilities and procedure as described in our recent article (21). For the visualization of *de novo* HSR generation (Figure 5), we transfected COLO 320DM cells expressing LacR-GFP fusion protein (6) with both pΔBN.AR1 and pSV2-8.32. Two days after transfection, the cells were suspended in growth medium containing 5 μg/ml of blasticidine and seeded into a 96 well glass-bottom dish (Iwaki, EZView culture plate LB) pre-coated with poly L-lysine (Sigma). The cells were viewed and photographed using an inverted microscope (Nikon TE 2000-E) with a 40× objective lens (Nikon ELWD plan fluor, NA 0.60) and a CCD camera (DS, Nikon) controlled by NIS-element software (Nikon). The images were exported from the NIS-element as a TIFF file, and processed using Adobe Photoshop CS version 8.0.1 (Adobe Systems Inc).

RESULTS

Detection of type 1 and type 2 structures in DMs or HSR

Transfection of human COLO 320DM cells with IR/MAR plasmids resulted in the generation of HSRs and/or DMs, as detected by FISH using the plasmid probe (Figure 1A). In this study, we used plasmids pSFVdhfr (Figure 1E), pΔBN.AR1, or pΔB.AR1 (Supplementary Figure S1) and blasticidine selection, as previously described (4,22). The polyclonal mixture of transformants included both the HSR-bearing and the DM-bearing cells (Figure 1B). Using PCR, we detected two types of recombined structures within the HSR and DMs. The 'type 1' structure is generated by re-joining two breaks inside the plasmid direct repeat, whereas the type 2 structure is the spaced inverted repeat (Figure 1C). For the detection of type 1, sets of forward and reverse primers several kilo base pairs apart were chosen. Thus, using a PCR reaction with a short extension time, amplification only occurred if the two primer sequences were close together, as in the type 1 structure (Figure 1C). For the detection of type 2 structure, primer sets in the same direction were chosen (Figure 1C). A representative image of the gel electrophoresis of the PCR product is shown in Supplementary Figure S2. Many bands appeared if total DNA from the HSR bearing cells was used as a template, whereas no band appeared if parental COLO 320DM cellular DNA mixed with pSFVdhfr plasmid DNA was used. Therefore, the PCR only amplified the recombined structure.

HSR had many type 1 and type 2 structures, whereas DMs had few type 1 and no type 2 structures

Sixty-four primers (Supplementary Table S1) along the entire plasmid sequence were synthesized (Supplementary Figure S1) and used as 140 and 75 primer sets (Supplementary Table S2) to specifically detect type 1 and type 2 structures, respectively. Using these primer sets, together with total DNA from the polyclonal transformants of plasmids pΔBN.AR1 or pΔB.AR1, PCR produced many bands representing type 1 or 2 structures (Figure 1D). The average number of such bands per primer set (y/x) suggested that the type 2 structure was more frequent than the type 1 structure (Figure 1D). Because the polyclonal transformants used in this experiment contained both DMs and HSRs (Figure 1B), we sought to establish a system that would enable analysis of DMs and HSRs separately. For this we used previously isolated cell clones that had DMs (clone 12) or HSRs (clone 22) as the sole site of gene amplification (4). Using DNA from clone 22, many type 1 and type 2 structures were detected. In contrast, markedly fewer type 1 structures and no type 2 structures were detected in DNA from DM-bearing clone 12 cells (Figure 1D). These results suggest that type 2 structures are restricted to the HSR, whereas type 1 structures may be generated in both DMs and HSRs, albeit with preferential accumulation in HSRs.

Type 1 or 2 junction appeared evenly throughout the entire plasmid sequence

To identify whether recombination in our experimental system is associated with specific sequence elements such as those involved in replication or transcription, we marked on the plasmid map the positions of the primers and their ability to generate a PCR product (Figure 1E and Supplementary Figure S3). The recombination points that generate the type 1 or 2 structure appeared to be evenly scattered throughout the plasmid sequence. However, type 1 recombination in DMs appeared to be biased to the replication initiation region from the *DHFR* locus (DHFR IR), especially at the sites that flank the transcription cassette ('α'and 'β' in the upper right-most panel in Figure 1E). This was consistent with our previous suggestion that the head-on collision between replication and transcription generates double-strand breakage (4).

Numerous type 1 and type 2 junctions exhibited microhomology

The PCR products developed above were sequenced to further characterize the nature of the junctions. Representative results are shown in Figure 2A. A substantial proportion of the PCR products [e.g. primer set (ps)-12 and Ps-176 in Figure 2A] contained a few bases overlap at type 1 or 2 junctions, suggesting that microhomology-mediated base pairing was involved in the generation of the structure. Structures with evidence of microhomology were detected at more than half of the

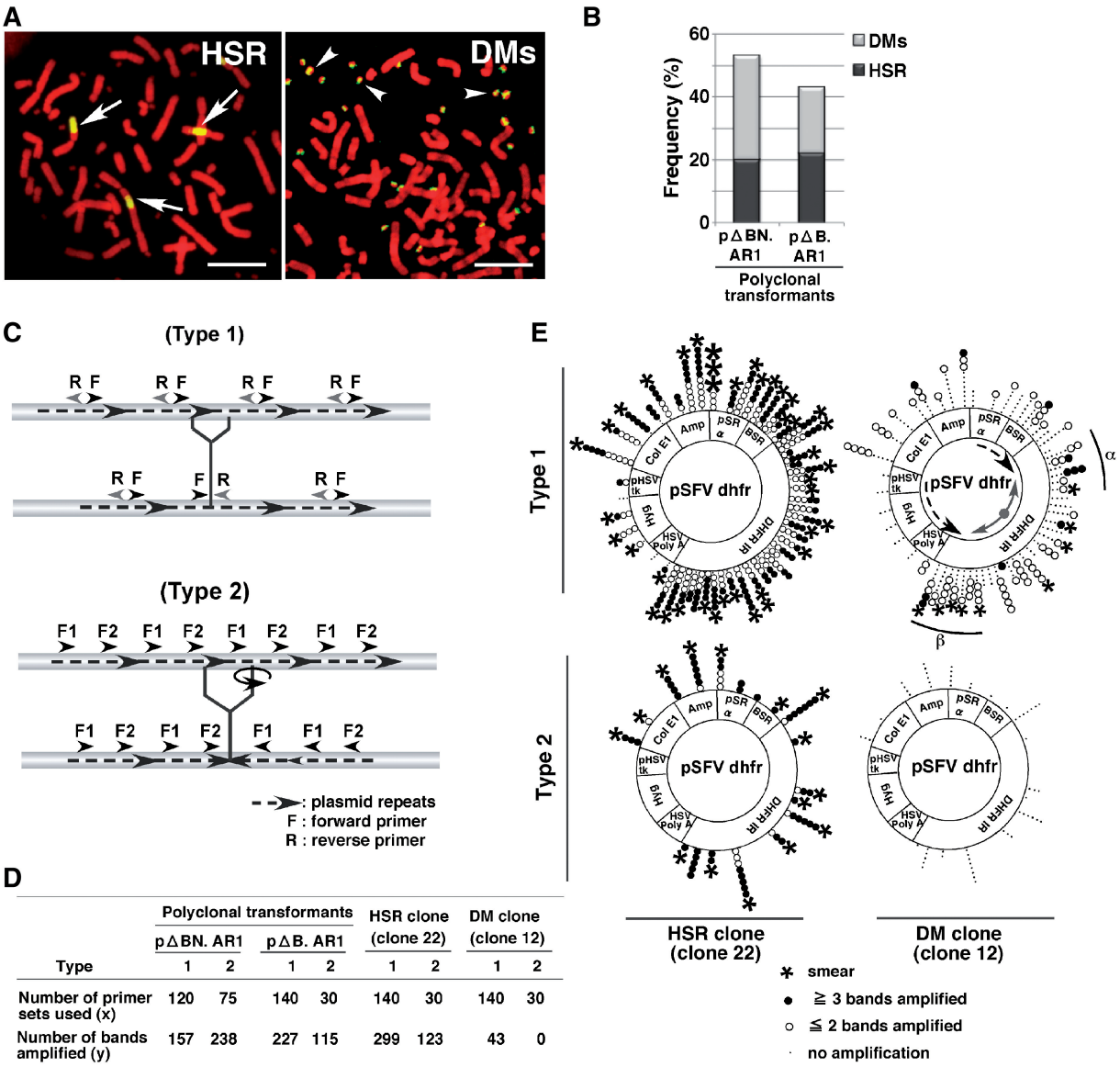

	Polyclonal transformants				HSR clone (clone 22)		DM clone (clone 12)	
	pΔBN. AR1		pΔB. AR1					
Type	1	2	1	2	1	2	1	2
Number of primer sets used (x)	120	75	140	30	140	30	140	30
Number of bands amplified (y)	157	238	227	115	299	123	43	0
y/x	1.3	3.2	1.6	3.8	2.1	4.1	0.3	0.0

Figure 1. Detection of type 1 and type 2 structures in amplified plasmid repeats. A representative image of HSRs (**A** left; arrow) and DMs (A right; arrowheads) generated by the IR/MAR plasmid in human COLO 320DM cells. The plasmid sequence was detected as green fluorescence after performing FISH with the plasmid probe on the chromosome spread, which was counterstained by PI (red). The frequency of the DM-bearing or HSR-bearing cells among the polyclonal mixture of transformed cells obtained by transfection with pΔBN.AR1 or pΔB.AR1 plasmid is shown in (**B**). In (**C**), the rationale for detecting type 1 or type 2 structures by PCR is depicted, where the dashed arrows represent the orientation of the plasmid repeats, and arrowheads represent the PCR primers. Comprehensive detection of type 1 or type 2 structures was undertaken by PCR using up to 140 or 75 primer sets, respectively (Supplementary Table S2). In (**D**), PCR was performed using primer sets that amplify type 1 or type 2 junctions and genomic DNA isolated from polyclonal pΔBN.AR1 transformants, pΔB.AR1 transformants, DMs-bearing clone 12 cells, or HSR-bearing clone 22 cells. The number of PCR primer sets used (x) and the number of product bands that appeared (y) were scored and listed together with the ratio between them (y/x). Primer sets that resulted in a smear on the gel were not included. In (**E**), the positions of primers that produced, in combination with another primer, no product (small dot), less than two bands (open circle), more than three bands (closed circle) or a smear (asterisk) were marked along the plasmid map of pSFVdhfr, which generated DMs or HSRs in clone 12 or clone 22, respectively. In the upper right-most panel in E, the orientation of the supposed replication fork (gray arrow) and transcription from the promoter (dashed arrow) is noted. In the same panel, the regions where type 1 junctions frequently appear are noted as 'α' and 'β'.

sequenced type 1 (22 out of 38) and type 2 (18 out of 29) junctions (Figure 2B). The remaining junctions that did not contain microhomology (Ps-6 and Ps-158 in Figure 2A) are likely to have been generated by blunt end ligation. Base insertion at the junction was not detected in any of the PCR products.

Use of bisulfite-modified PCR revealed the structure of inverted repeats including the detection of perfect palindromes

The type 2 structures described so far in this study are spaced inverted repeats. This is because PCR cannot amplify an inverted repeat without a space, i.e. a perfect

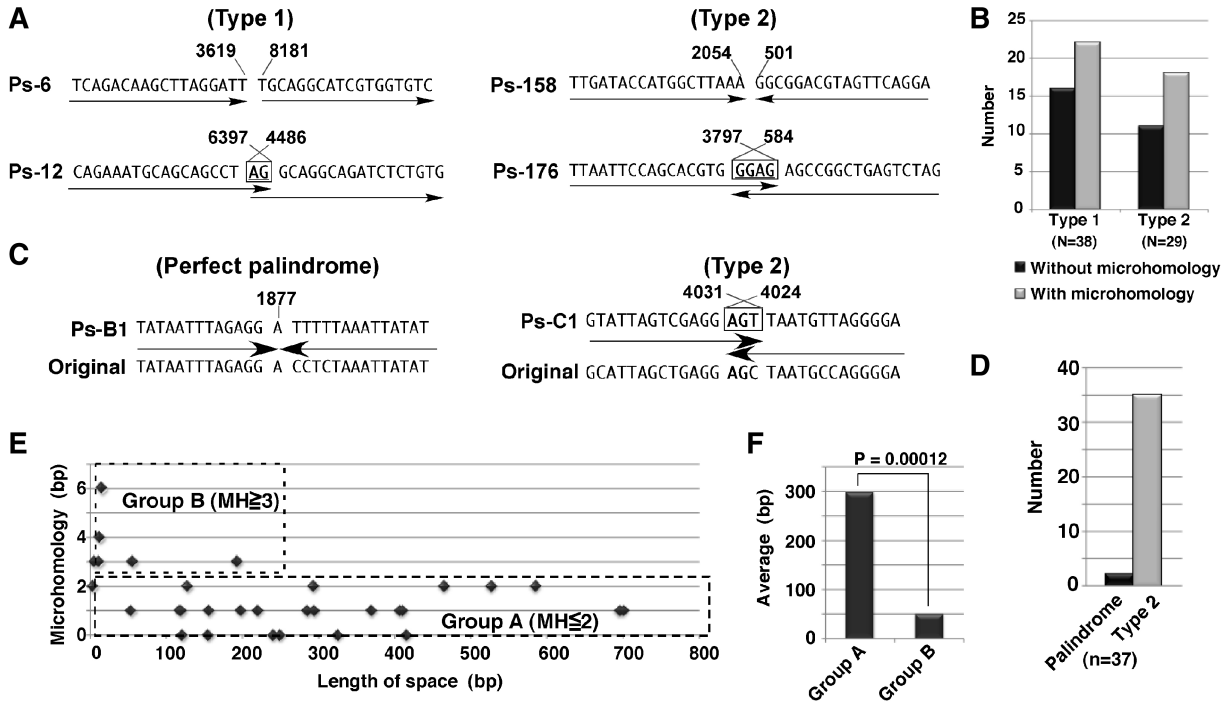

Figure 2. Features of type 1 and type 2 junctions. The PCR products obtained in Figure 1D were cloned in *E. coli* and sequenced. Representative sequences for type 1 and type 2 structures are shown in **A**. Arrows indicate the orientation of the sequence. More than half of the type 1 or type 2 junctions included microhomology; the incidence of which is shown in **B**. To amplify perfect palindromes or inverted repeats with short spaces, template DNA was treated with bisulfite and subjected to PCR using specially designed primers (Supplementary Table S4). PCR products were cloned into *E. coli* and the representative sequences around the junctions are shown in (**C**). This analysis revealed the presence of perfect palindromes. The number of such palindromes, together with the number of corresponding spaced inverted repeats (Type 2), are shown in **D**. For such inverted repeats, the length of space between the repeats was plotted against the length of microhomology (**E**). We divided these events into two groups: group A, with <2 bp microhomology, and group B, with >3 bp microhomology. The average length of space between the repeats of these two groups was significantly different ($P = 0.00012$ by student's *t*-test; **F**).

palindrome, even if it is present. Therefore, we treated the template DNA with bisulfite to convert unmethylated cytosines to uracils. This strategy was used by us to successfully remove a palindromic sequence in a previous study (20), thereby facilitating PCR amplification. The resulting DNA was subjected to PCR using four specially designed primer sets (a to d in Supplementary Figure S1 and Supplementary Table S4). Numerous PCR bands were obtained using template derived from the polyclonal transformant or the HSR-bearing clone 22 cell (Supplementary Figure S4). These PCR products were sequenced, and 2 out of 37 sequences contained perfect palindromes (Figure 2C and D). All of the other sequences were conventional type 2 structures with a spaced, inverted repeat. The junctions contained much shorter spaces than those shown in Figure 2, as calculated by subtracting the position numbers at the junction. Most of the junctions also contained microhomologies. Therefore, we plotted the length of the space against the length of the microhomology (Figure 2E). The results suggested that the longer microhomology regions ('Group B') were more frequently associated with shorter space lengths (Figure 2F). This will be discussed in the following section.

We found a case in which three type 2 junctions appeared in perfect symmetry (Figure 3A). The generation of such symmetrical structures may not be explained by simple non-homologous end joining (NHEJ), but it may be explained by the mechanism depicted in Figure 3B. This will be discussed in relation to how the type 2 junction could have been generated in a chromosomal context.

Using template DNA derived from the DM-bearing clone 12, the bisulfite-modified PCR produced type 2 bands only if primer set 'c' was used (Supplementary Figure S4). We sequenced the junctions of these bands and found that all three obtained sequences were different from the usual type 2 structures, featuring a short inverted repeat flanking the junction of a large inverted repeat (Figure 3C and Supplementary Figure S5). We hereafter designate such junctions as 'type 2*'. Notably, a short inverted repeat frequently appears at the center of the DHFR replication initiation region, corresponding to the location of primer set 'c' (Supplementary Figure S1). The most plausible explanation for how the type 2* junction appears is depicted in Figure 3C. In the following section, this will be discussed in relation to the elimination of most of the junctions in the extrachromosomal context.

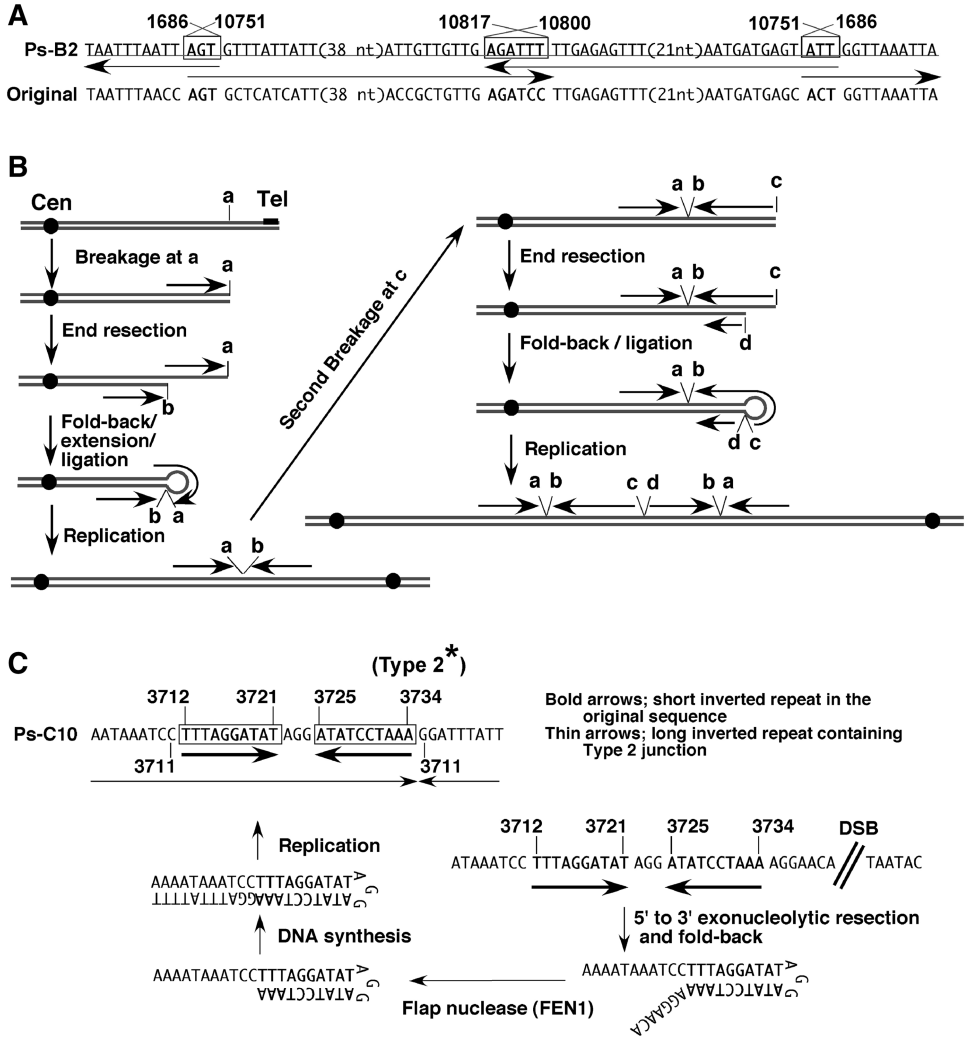

Figure 3. Inverted repeat found in HSRs and DMs and models that may explain its generation. The sequence analysis shown in Figure 2 revealed a case in which three type 2 junctions were arranged symmetrically in HSRs (**A**). A plausible model of how such a structure might arise is depicted in (**B**). The bisulfite-modifed PCR using DM-bearing clone 12 cells produced only a few bands (Supplementary Figure S4). All three sequences [(**C**) and Supplementary Figure S5] had a unique feature: a large inverted repeat (horizontal thin arrows) was flanked by a short inverted repeat (horizontal bold arrows). A plausible model describing how such a structure could be generated is depicted in the same panel.

Inverted repeats were associated with the generation of a longer HSR

Inverted repeats were found frequently in the HSR (see above). Next, we examined the effect of inverted repeats in the IR/MAR plasmid on HSR generation, as gene amplification was suggested to be enhanced in yeast cells (23). Several plasmids, each differing in the nature of the inserted *Alu* repeats (Figure 4A), were transfected alone or together with a plasmid expressing d2EGFP protein into COLO 320DM cells. Co-transfection with IR/MAR plasmid always resulted in co-amplification of the co-transfected sequences (4). As a result, the *Alu* inverted repeat resulted in the generation of a longer HSR, whereas the direct repeat or single *Alu* had no apparent effect on HSR length, compared with the pΔBN.AR1 control plasmid (Figure 4B). Protein expression from the amplified region was evaluated by measuring the fluorescence intensity of the d2EGFP protein, and was not affected by the progression of gene amplification (Figure 4C). This will be discussed later.

Live-cell observations of chromatin bridge breaks

To extend the above study, we observed how the HSRs behaved in live cells. For this purpose, we had previously isolated 'HSR-GFP' (6) and 'HSR-CFP' (10) cell clones. Namely, we amplified a lactose operator (LacO) repeat as a HSR by using the IR/MAR plasmid. The HSR tagged with LacO repeat was visualized by the binding of lactose repressor (LacR)-GFP or CFP fusion protein (Supplementary Figure S6). In this study, the 'HSR-CFP' cell clone was used. Time-lapse observations of more than 10 events of anaphase bridge breakage showed that the bridge broke almost in the middle every time, and that breakage occurred during anaphase

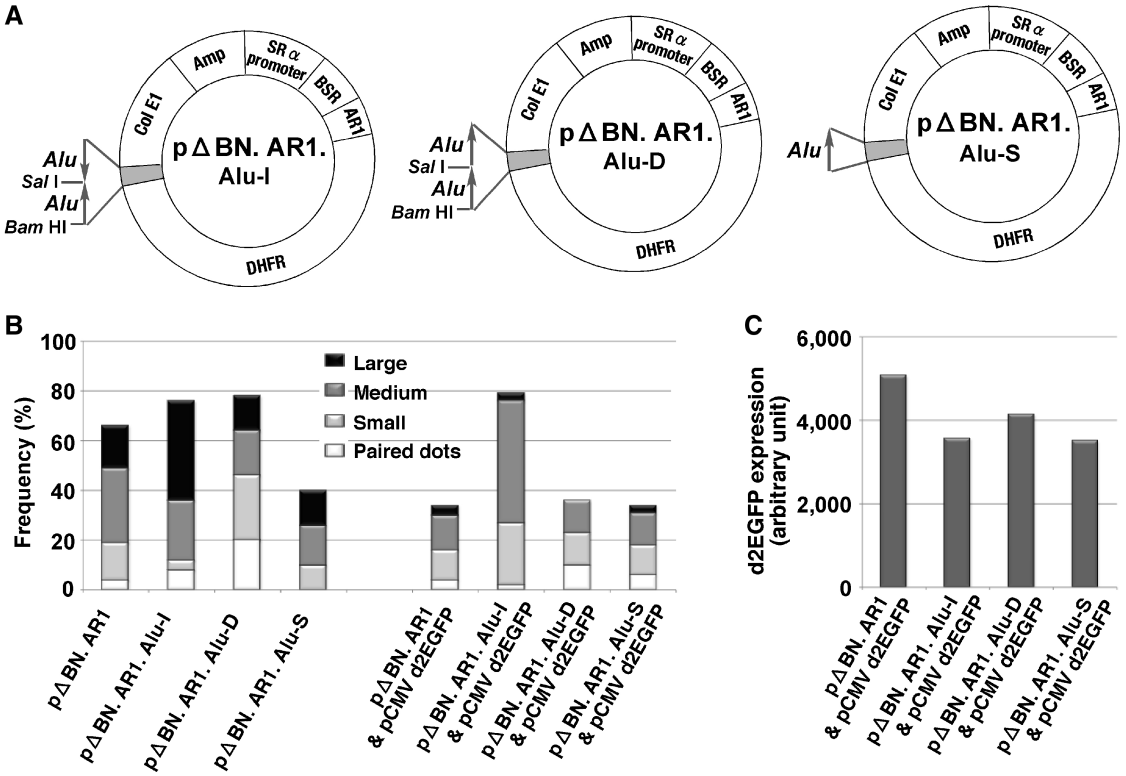

Figure 4. The inverted repeat was associated with the generation of a longer HSR. COLO 320DM cells were transfected with the pΔBN.AR1 plasmid or the plasmids with Alu sequences (**A**), without (left part of B) or with (right part of **B** and **C**) pCMV-d2EGFP plasmid. Co-transfected plasmids have been shown to co-amplify with the IR/MAR plasmid (4). The metaphase chromosome spread was prepared from stable transformants and was examined by FISH using plasmid probes. The frequency of cells bearing HSRs of varying size among the metaphase cells is plotted in B. The size of the HSR was evaluated by comparing chromosome width and was arbitrarily expressed as 'paired dots' to 'large' (more than twice the chromosome width), as done previously (20). The expression of the d2EGFP protein was measured by flow cytometry, as done previously (7).

progression (Figure 5A and Supplementary Video S1). These results are consistent with those of our previous article (6). However, in one case, the bridge was severed in the middle during cytokinesis (Figure 5B), which suggested that if the bridge is too long to be severed by spindle shortening or spindle pole movement, it may be severed by the contraction of the contractile ring. Furthermore, the bridge may not be broken if it might be too long to be severed. In such case, the cell became bi-nucleated (Supplementary Figure S7), probably because the unbroken bridge inhibited the completion of cytokinesis (6,24). This suggests that mechanical tension from the spindle caused the bridge to sever in the middle, and, importantly, that breakage in the middle may not cause elongation of the HSR in accordance with the classical BFB cycle model. This will be further discussed in the following section.

De novo HSR generation was more rapid than predicted by the BFB cycle model

We next observed *de novo* HSR generation in live cells. Namely, we co-transfected the IR/MAR plasmid and the LacO plasmids into COLO 320DM cells expressing LacR-GFP, as before (Supplementary Figure S6). Transformants were grown in a 96-well glass bottom dish under blasticidine selection, and were carefully observed using fluorescence microscopy. Surprisingly, among the small colonies that arose only 7 days after the transfection, bright GFP spots appeared sporadically in the nucleus of living cells (Figure 5C). The appearance of these spots was highly similar to those in the previous experiment, where FISH proved the GFP spots were actually HSR (6). The number of such spots per colony increased between 1 week and 3 weeks (Figure 5E). Among such GFP spots, we observed an unbroken chromatin bridge between two cells (Figure 5D, inset), which was very similar to the unbroken chromatin bridge image shown in Supplementary Figure S7 or in our previous article (6). Therefore, we regarded the nuclear GFP spots as HSR. The size of the GFP spot was roughly similar to the one of the HSR composed of more than a thousand copies of plasmid sequence, e.g. that appeared in Figure 5A and B. Because the doubling time for these cells is about 24 h (data not shown), the cells should divide only seven times at most after transfection. This was far more rapid than predicted by the classical BFB cycle model.

Massive DNA synthesis was detected at the broken chromatin bridge during the G1 to S phase transition

A possible mechanism for rapid HSR lengthening could involve DNA synthesis at the broken end. To verify this

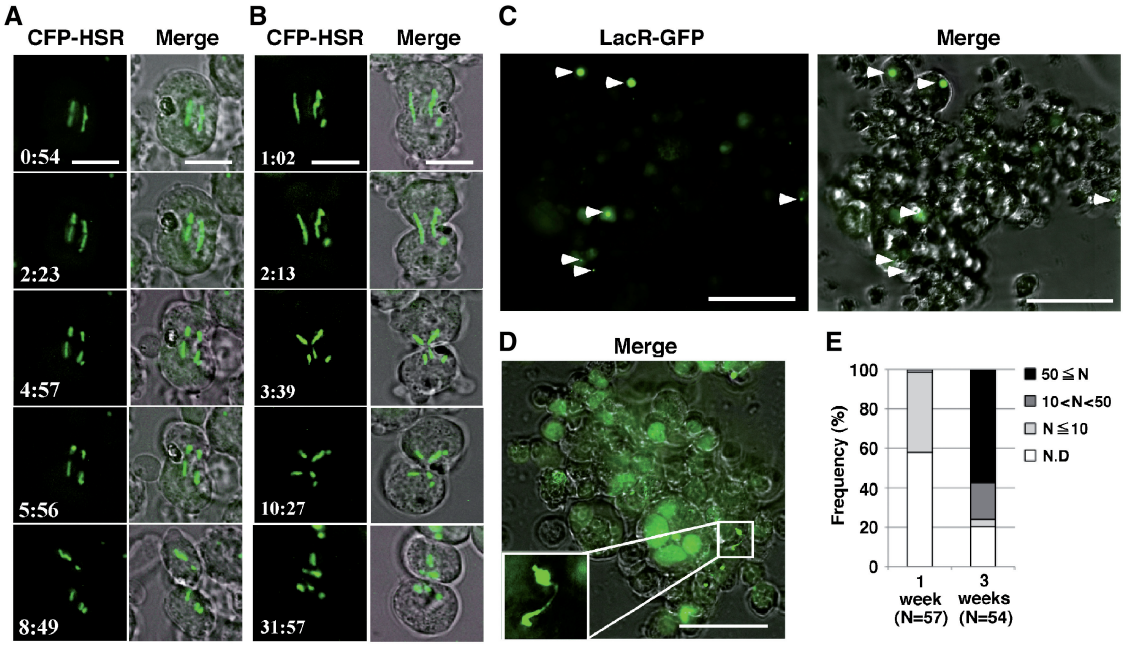

Figure 5. Live cell observation of cell behavior and generation of HSRs. Examples of time-lapse observations of HSR-CFP cells during mitosis are shown in (**A**) and (**B**). Both the fluorescence image (left) and the same image merged to the differential inference contrast (DIC) image (right) are shown. The time is in minutes and seconds. Each bar represents 10 μm. A plasmid bearing the LacO repeat (pSV2-8.32) was amplified as HSR by using IR/MAR plasmid in COLO 320DM cells that express LacR-GFP protein. In the primary colony formed by the transformants, we could detect HSR at only 7 days after the transfection (**C**). Among such HSRs, an anaphase chromatin bridge was observed (**D**, inset). Scale bars represent 50 μm. In (**E**), the number of HSR spots (N) per colony was counted at 1 or 3 weeks after the transfection.

possibility, we partially synchronized the cell cycle of HSR-CFP cells with nocodazole, which arrests cells in prometaphase, and then released the cells into fresh medium and treated them with BrdU. We then fixed the cells and detected the incorporated BrdU. Surprisingly, the BrdU signal was particularly bright at an HSR that appeared as a nuclear protrusion (Figure 6A–C; yellow arrows). Our previous time-lapse observation showed that such HSRs, in these sorts of nuclear protrusions, were remnants of broken chromatin bridges [Figure 5, Supplementary Video S1 and Figures appearing in Shimizu *et al.* (6)]. We observed 418 such broken HSRs, and 413 of them exhibited BrdU signals. On the other hand, no BrdU signals were detected in any of the HSRs inside the nucleus (388/388) (Figure 6A–C; white arrowheads), even if they were in the same cell with the BrdU-positive broken HSR. BrdU-positive broken HSRs were detected in both BrdU-negative [HSR(+)/N(); Figure 6A and B] and BrdU-positive (HSR(+)/N(+); Figure 6C) nuclei. This suggested that BrdU-positive HSRs may exist both in non-S and S phase cells. Because we partially synchronized the cell cycle, the fraction of M phase cells decreased and the fraction of BrdU-positive S phase cells increased as time progressed after release from the nocodazole (Figure 6D). At that time, the fraction of HSR(+)/N(–) cells increased and then decreased, whereas the population of HSR(+)/N(+) cells increased only (Figure 6E). These results suggested that DNA synthesis at the broken HSR continued during the transition from G1 to S phase.

DISCUSSION

In this study we have identified the nature of recombination in the amplified region, and have observed how HSRs are generated and maintained in live cells. We clearly showed that the unscheduled replication seen at the nuclear protrusion occurred at a broken anaphase bridge. These data, combined with our previous data, serve to significantly advance our understanding of how gene amplification progresses, as described below.

Appearance of type 1 and type 2 junctions in HSRs

We detected numerous type 1 and type 2 structures in the HSRs. We showed previously that the IR/MAR plasmid is first amplified to generate a direct repeat (4). Therefore, the generation of the type 1 structure, a truncated direct repeat, appears to be simple. Namely, the most plausible explanation is that NHEJ of two broken ends inside the plasmid direct repeat generated the structure (Figure 7A and B). On the other hand, generation of the type 2 structure, a spaced inverted repeat, is not as simple. It might be possible that the NHEJ process also generated the type 2 structure, but an important observation countering this idea was the appearance of a structure in which three type 2 junctions with microhomologies were arranged in perfect symmetry (Figure 3A). Such a structure would not be explained by NHEJ, and the only conceivable mechanism would have to include the generation of a hairpin-end by fusion of the broken ends (Figures 3B and 7A). Namely, if the double-strand breakage arose from inside the plasmid repeat, it would be followed by a 5′ to 3′

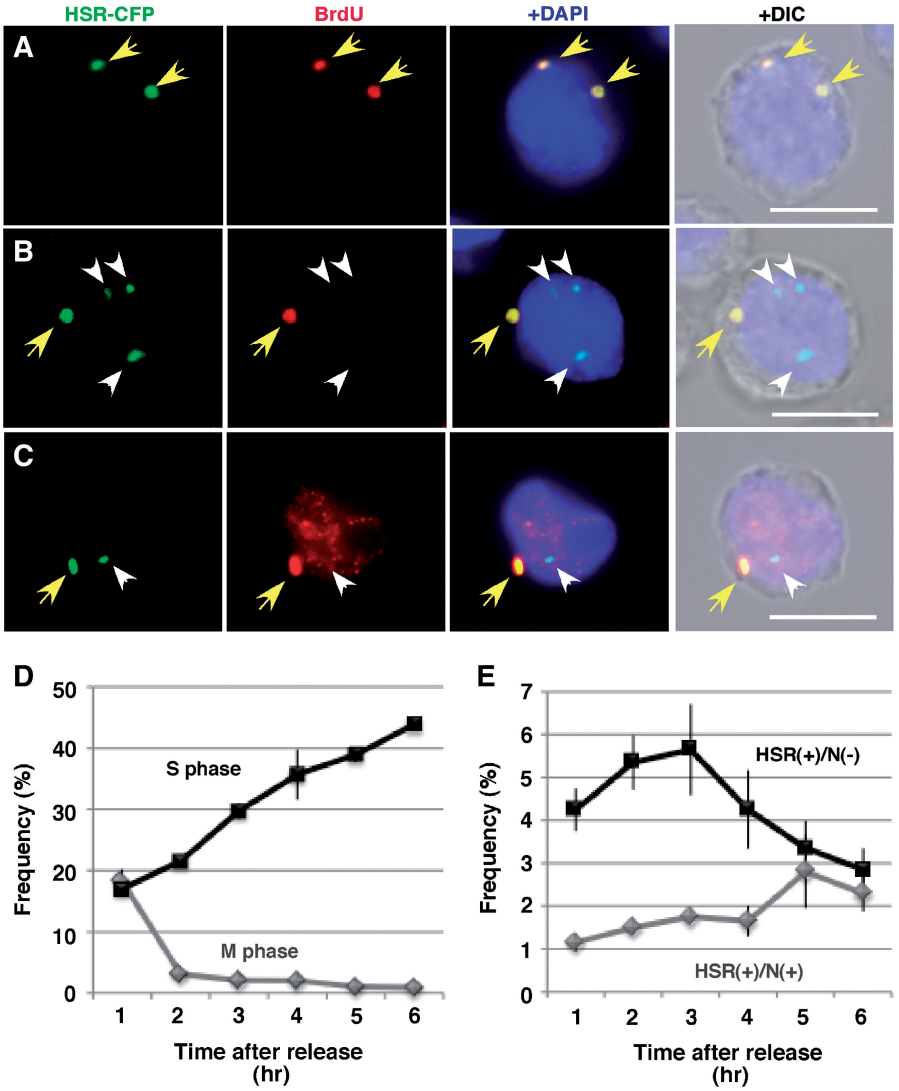

Figure 6. Detection of DNA synthesis at the broken chromatin bridge. The cell cycles of HSR-CFP cells were partially synchronized by nocodazole treatment (10 h). Cells were then released into fresh medium for the indicated time. BrdU was added to the culture 1 h before harvest. The incorporated BrdU was detected by BrdU-specific antibodies in red fluorescence, and nuclear DNA was counterstained by DAPI in blue. Three representative photos are shown in (**A**), (**B**) and (**C**). The HSR at the nuclear protrusion is a remnant of a broken chromatin bridge, and it incorporated BrdU 100% of the time (yellow arrow), while the HSR inside the nucleus did not incorporate BrdU (white arrowhead). Scale bar represents 10 μm. The frequencies of the mitotic and S phase cells were obtained by examining more than 500 cells for each time point, and they are shown in (**D**). The mitotic cells were identified by DAPI staining, and the S phase cells were identified by BrdU incorporation in the nucleus. We scored the frequencies of the cells in which BrdU was detected only at the broken HSR [HSR(+)N(–)]and the cells in which BrdU was detected both at the broken HSR and in the nucleus [HSR(+)N(–)] by examining more than 500 cells for each time point, three times each. The resulting percentages are plotted in E.

exonucleolytic resection, and the single-stranded product would be folded back using microhomology at the 3′ end. Extension of this product by DNA polymerase would generate a hairpin end that may be converted to a dicentric chromatid after replication of the entire chromosome. A similar mechanism, involving a short inverted repeat instead of microhomology, was previously suggested to account for the generation of dicentric chromatids (25,26). If the second breakage were to occur in the proximity of the first one, the repetition of the previous cycle would generate the symmetrical arrangement of three type 2 junctions, as we observed (Figure 3B). This observation therefore strongly suggested that this mechanism is responsible for the generation of type 2 junctions in this context. Our finding of palindromic sequences also suggested that the broken end may directly fuse to form a hairpin end.

How does the HSR elongate?

The above hairpin-end-mediated mechanism may generate dicentric chromatids after replication, in a chromosomal context (Figures 3B and 7A). On the other hand, recent studies in yeast cells have shown that the nearby inverted repeat can also fuse to generate a dicentric chromatid through a replication-based mechanism without break-formation (27,28). Such a dicentric chromatid would be

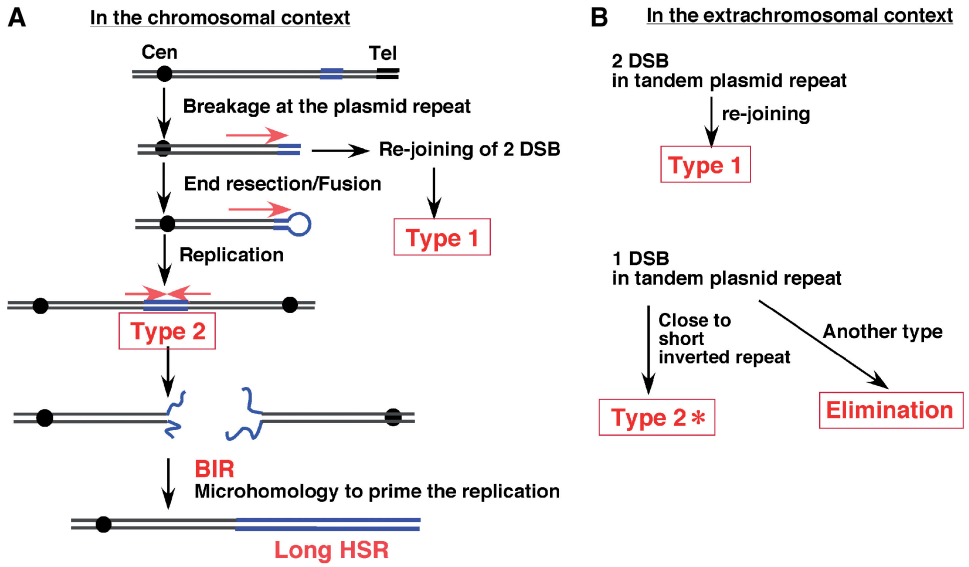

Figure 7. Model for gene amplification mediated by the IR/MAR-bearing plasmid in chromosomal and extrachromosomal contexts. (**A**) The generation of type 1 and type 2 junctions after double-strand breakage (DSB) in the chromosomal context: generation of a dicentric chromatid and a broken bridge induces replication, and this extends HSR length. Red arrows represent the orientation of the sequence, blue lines represent the plasmid sequence, and black circles represent the centromere. (**B**) A specific type of repair product may remain in the extrachromosomal context while another type of DSB may be eliminated.

expected to appear as an anaphase chromatin bridge. Our studies demonstrated the formation of just such a bridge.

Since the classical BFB cycle model proposes that bridge breakage results in unequal segregation of genes near the breakage to daughter cells, the gene copy number may increase. However, we found that the bridge usually broke near the middle [Figure 5A and B and Shimizu *et al.* (6)], so the number of genes would scarcely be expected to change during one division. On the other hand, our observations of live cells suggested rapid generation of HSRs, with roughly one thousand copies of the 10-kb plasmid being generated in less than seven cell divisions (Figure 5C–E). The classical BFB model does not adequately explain these observations.

On the other hand, we have demonstrated massive unscheduled replication at the broken chromatin bridge during the G1 to S phase transition. These results are consistent with those of recent studies, which suggested a mechanism involving break-induced replication (BIR) for gene amplification and gross chromosomal alteration in yeast and mammalian cells (29–32). Our current result showing bright BrdU labeling at the broken HSR is the most striking evidence for BIR in mammalian cells, thus far. Furthermore, it is the first report of BIR at a specific site, i.e. the nuclear protrusion. Most plausibly, the broken end of the anaphase bridge may prime the BIR (Figure 7B). The 'broken-bridge initiated BIR' had been hypothesized in yeast cells (33). Namely, the 3′ single-strand end may form a D-loop and initiate BIR by using microhomology (30). At that time, it may anneal to itself or to the complementary strand using microhomology. Extension of the strand by BIR may generate the elongated HSR at the chromosome end. Importantly, the product should contain a type 2 or type 1 junction. Therefore, this model provides a plausible explanation for the accumulation of type 1 and type 2 structures in HSR. The mechanism may also explain the generation of chromosomal ladder type HSR in which plasmid repeats are arranged as an orderly spaced ladder (6), which has been regarded as the hallmark of the BFB cycle (34,35). This would occur if the D-loop was formed at the genomic region adjacent to the plasmid repeat.

The presence of an *Alu* inverted repeat in the IR/MAR plasmid enhanced HSR generation (Figure 4). The enhancement of gene amplification by inverted repeats has been reported in yeast cells (33,36). The shortly spaced inverted repeat could readily generate a dicentric chromatid by a mechanism involving strand breakage [Figure 3C and (25,26)], or by a replication-based mechanism without breakage (27,28). We showed that the HSR included palindromic sequences as well as shortly spaced inverted repeats (Figure 2C and D). These may contribute to the elongation of the HSR. Interestingly, protein expression was not increased despite the increase in gene number (Figure 4C). We speculate that the RNA from the inverted repeat may fold back and produce double-stranded RNA leading to RNA interference and silencing of the cognate sequence.

Differences between the extrachromosomal and the chromosomal context

In DMs, a low frequency of type 1 structures, and, essentially, a lack of typical type 2 structures, were observed. This finding is consistent with our previous report that most DMs were composed of ordered direct repeats (4).

The only inverted repeat found in DMs was type 2* in structure and was located adjacent to the short inverted

repeat (Figure 3C). This may be explained by the generation of single-stranded DNA followed by folding-back on the short inverted repeat (Figure 3C). The excess nucleotide could have been degraded by a flap nuclease such as FEN1, which would have then produced a large inverted repeat through DNA synthesis. The Ps-C10 sequence (Figure 3C) contained a 10-bp short inverted repeat with a 3-bp space, both of which were derived from the original plasmid sequence. Interestingly, such a short inverted repeat may be regarded as an extraordinarily long microhomology with a short space; thus, the type 2* structure may be an extreme case of the type 2 structure. Our results suggested that longer microhomology is more frequently associated with shorter spacing (Figure 2E). This may suggest that longer regions of microhomology are more stable and therefore rapidly repaired. We previously reported that DMs might undergo aggregation and elimination from cells if the DNA damage in the DMs was induced by a low concentration of a replication inhibitor such as hydroxyurea (8). Therefore, we suggest that the microhomology-mediated repair process (normal type 2) in DMs might be linked to their aggregation and elimination from the cells, while the inverted repeat-mediated repair process (type 2*), which probably proceeds more rapidly, might not be linked to their elimination. Thus, only the type 2* structure may remain in DMs.

SUPPLEMENTARY DATA

Supplementary Data are available at NAR Online.

ACKNOWLEDGEMENTS

The authors thank Dr Kirill Lobachev for his kind gift of plasmid pHS-I and pHS-D.

FUNDING

Grant-in-Aid for Scientific Research (B) [grant number 17370002] and Grant-in-Aid for Challenging Exploratory Research [grant number 21657051] from the Japan Society for the Promotion of Science (to N.S.); Grant-in-Aid for Scientific Research on Priority Areas—Nuclear dynamics [grant number 19038016] from the Ministry of Education, Science, Sports and Culture of Japan (to N.S.). Funding for open access charge: Grant-in-Aid for Challenging Exploratory Research [grant number 21657051].

Conflict of interest statement. None declared.

REFERENCES

1. Albertson,D.G. (2006) Gene amplification in cancer. *Trends Genet*., **22**, 447–455.
2. Shimizu,N. (2009) Extrachromosomal double minutes and chromosomal homogeneously staining regions as probes for chromosome research. *Cytogenet. Genome Res*., **124**, 312–326.
3. Wahl,G.M. (1989) The importance of circular DNA in mammalian gene amplification. *Cancer Res*., **49**, 1333–1340.
4. Shimizu,N., Hashizume,T., Shingaki,K. and Kawamoto,J.K. (2003) Amplification of plasmids containing a mammalian replication initiation region is mediated by controllable conflict between replication and transcription. *Cancer Res*., **63**, 5281–5290.
5. Shimizu,N., Ochi,T. and Itonaga,K. (2001) Replication timing of amplified genetic regions relates to intranuclear localization but not to genetic activity or G/R band. *Exp. Cell Res*., **268**, 201–210.
6. Shimizu,N., Shingaki,K., Kaneko-Sasaguri,Y., Hashizume,T. and Kanda,T. (2005) When, where and how the bridge breaks: anaphase bridge breakage plays a crucial role in gene amplification and HSR generation. *Exp. Cell Res*., **302**, 233–243.
7. Shimizu,N., Hanada,N., Utani,K. and Sekiguchi,N. (2007) Interconversion of intra- and extra-chromosomal sites of gene amplification by modulation of gene expression and DNA methylation. *J. Cell. Biochem*., **102**, 515–529.
8. Shimizu,N., Misaka,N. and Utani,K. (2007) Nonselective DNA damage induced by a replication inhibitor results in the selective elimination of extrachromosomal double minutes from human cancer cells. *Genes, Chrom. Cancer*, **46**, 865–874.
9. Utani,K., Kawamoto,J.K. and Shimizu,N. (2007) Micronuclei bearing acentric extrachromosomal chromatin are transcriptionally competent and may perturb the cancer cell phenotype. *Mol. Cancer Res*., **5**, 695–704.
10. Utani,K. and Shimizu,N. (2009) How transcription proceeds in a large artificial heterochromatin in human cells. *Nucleic Acids Res*., **37**, 393–404.
11. Shimizu,N. and Shingaki,K. (2004) Macroscopic folding and replication of the homogeneously staining region in late S phase leads to the appearance of replication bands in mitotic chromosomes. *J. Cell Sci*., **117**, 5303–5312.
12. Bosisio,D., Marazzi,I., Agresti,A., Shimizu,N., Bianchi,M.E. and Natoli,G. (2006) A hyper-dynamic equilibrium between promoter-bound and nucleoplasmic dimers controls NF-kappaB-dependent gene activity. *EMBO J*., **25**, 798–810.
13. Tanaka,T. and Shimizu,N. (2000) Induced detachment of acentric chromatin from mitotic chromosomes leads to their cytoplasmic localization at G1 and the micronucleation by lamin reorganization at S phase. *J. Cell Sci*., **113**, 697–707.
14. McClintock,B. (1951) Chromosome organization and genic expression. *Cold Spring Harbor Symp. Quant. Biol*., **16**, 13–47.
15. Tanaka,H. and Yao,M.C. (2009) Palindromic gene amplification–an evolutionarily conserved role for DNA inverted repeats in the genome. *Nat. Rev. Cancer*, **9**, 216–224.
16. Haber,J.E. and Debatisse,M. (2006) Gene amplification: yeast takes a turn. *Cell*, **125**, 1237–1240.
17. Bailey,S.M. and Murnane,J.P. (2006) Telomeres, chromosome instability and cancer. *Nucleic Acids Res*., **34**, 2408–2417.
18. Lobachev,K.S., Gordenin,D.A. and Resnick,M.A. (2002) The Mre11 complex is required for repair of hairpin-capped double-strand breaks and prevention of chromosome rearrangements. *Cell*, **108**, 183–193.
19. Shimizu,N., Kanda,T. and Wahl,G.M. (1996) Selective capture of acentric fragments by micronuclei provides a rapid method for purifying extrachromosomally amplified DNA. *Nat. Genet*., **12**, 65–71.
20. Harada,S., Uchida,M. and Shimizu,N. (2009) Episomal high copy number maintenance of hairpin-capped DNA bearing a replication initiation region in human cells. *J. Biol. Chem*., **284**, 24320–24327.
21. Utani,K., Kohno,Y., Okamoto,A. and Shimizu,N. (2010) Emergence of micronuclei and their effects on the fate of cells under replication stress. *Plos ONE*, **5**, e10089.
22. Shimizu,N., Miura,Y., Sakamoto,Y. and Tsutsui,K. (2001) Plasmids with a mammalian replication origin and a matrix attachment region initiate the event similar to gene amplification. *Cancer Res*., **61**, 6987–6990.
23. Narayanan,V. and Lobachev,K.S. (2007) Intrachromosomal gene amplification triggered by hairpin-capped breaks requires homologous recombination and is independent of nonhomologous end-joining. *Cell cycle*, **6**, 1814–1818.
24. Huang,H., Fletcher,L., Beeharry,N., Daniel,R., Kao,G., Yen,T.J. and Muschel,R.J. (2008) Abnormal cytokinesis after X-irradiation

in tumor cells that override the G2 DNA damage checkpoint. *Cancer Res.*, **68**, 3724–3732.
25. Tanaka,H., Tapscott,S.J., Trask,B.J. and Yao,M.C. (2002) Short inverted repeats initiate gene amplification through the formation of a large DNA palindrome in mammalian cells. *Proc. Natl Acad. Sci. USA*, **99**, 8772–8777.
26. Okuno,Y., Hahn,P.J. and Gilbert,D.M. (2004) Structure of a palindromic amplicon junction implicates microhomology-mediated end joining as a mechanism of sister chromatid fusion during gene amplification. *Nucleic Acids Res.*, **32**, 749–756.
27. Paek,A.L., Kaochar,S., Jones,H., Elezaby,A., Shanks,L. and Weinert,T. (2009) Fusion of nearby inverted repeats by a replication-based mechanism leads to formation of dicentric and acentric chromosomes that cause genome instability in budding yeast. *Genes Dev.*, **23**, 2861–2875.
28. Mizuno,K., Lambert,S., Baldacci,G., Murray,J.M. and Carr,A.M. (2009) Nearby inverted repeats fuse to generate acentric and dicentric palindromic chromosomes by a replication template exchange mechanism. *Genes Dev.*, **23**, 2876–2886.
29. Watanabe,T. and Horiuchi,T. (2005) A novel gene amplification system in yeast based on double rolling-circle replication. *EMBO J.*, **24**, 190–198.
30. Hastings,P.J., Ira,G. and Lupski,J.R. (2009) A microhomology-mediated break-induced replication model for the origin of human copy number variation. *PLoS genet.*, **5**, e1000327.
31. Ruiz,J.F., Gomez-Gonzalez,B. and Aguilera,A. (2009) Chromosomal translocations caused by either pol32-dependent or pol32-independent triparental break-induced replication. *Mol. Cell. Biol.*, **29**, 5441–5454.
32. Zhang,F., Carvalho,C.M. and Lupski,J.R. (2009) Complex human chromosomal and genomic rearrangements. *Trends Genet.*, **25**, 298–307.
33. Narayanan,V., Mieczkowski,P.A., Kim,H.M., Petes,T.D. and Lobachev,K.S. (2006) The pattern of gene amplification is determined by the chromosomal location of hairpin-capped breaks. *Cell*, **125**, 1283–1296.
34. Selvarajah,S., Yoshimoto,M., Park,P.C., Maire,G., Paderova,J., Bayani,J., Lim,G., Al-Romaih,K., Squire,J.A. and Zielenska,M. (2006) The breakage-fusion-bridge (BFB) cycle as a mechanism for generating genetic heterogeneity in osteosarcoma. *Chromosoma*, **115**, 459–467.
35. Marella,N.V., Zeitz,M.J., Malyavantham,K.S., Pliss,A., Matsui,S., Goetze,S., Bode,J., Raska,I. and Berezney,R. (2008) Ladder-like amplification of the type I interferon gene cluster in the human osteosarcoma cell line MG63. *Chrom. Res.*, **16**, 1177–1192.
36. Lobachev,K.S., Stenger,J.E., Kozyreva,O.G., Jurka,J., Gordenin,D.A. and Resnick,M.A. (2000) Inverted Alu repeats unstable in yeast are excluded from the human genome. *EMBO J.*, **19**, 3822–3830.